Blockchain and Computational Intelligence Inspired Incentive-Compatible Demand Response in Internet of Electric Vehicles

Zhenyu Zhou, *Senior Member, IEEE*, Bingchen Wang, Yufei Guo, and Yan Zhang, *Senior Member, IEEE*

***Abstract*—By leveraging the charging and discharging capabilities of Internet of electric vehicles (IoEV), demand response (DR) can be implemented in smart cities to enable intelligent energy scheduling and trading. However, IoEV-based DR confronts many challenges, such as a lack of incentive mechanism, privacy leakage, and security threats. This motivates us to develop a distributed, privacy-preserved, and incentive-compatible DR mechanism for IoEV. Specifically, we propose a consortium blockchain-enabled secure energy trading framework for electric vehicles (EVs) with moderate cost. To incentivize more EVs to participate in DR, a contract theory-based incentive mechanism is proposed, in which various contract items are tailored for the unique characteristics of EV types. The contract optimization problem falls into the category of difference of convex programing, and is solved by using the iterative convex–concave procedure algorithm. Furthermore, we consider the scenario where the statistical knowledge of the EV type is unknown. In such a case, we demonstrate how to derive the probability distribution of the EV type by exploring computational intelligence-based state of charge estimation techniques, e.g., Gaussian process regression. Finally, the security and efficiency performance of the proposed scheme is analyzed and validated.**

***Index Terms*—Demand response, consortium blockchain, machine learning, contract theory, Internet of electric vehicles, computational intelligence.**

I. Introduction

A. Background and Motivation

SMART energy management, which enables the utilization of the scarce energy resources in an optimal manner, is essential to build a smart, green, and sustainable city [1], [2]. However, the large-scale penetration of intermittent distributed renewable energy sources and uncoordinated electric vehicles (EVs) poses new challenges on smart energy management. Specifically, in order to balance load and supply, a large number of centralized generators and energy storage devices have to be deployed [3], which results in significant capital expenditure (CAPEX) and operational expenditure (OPEX). An alternative way is to explore the rapid proliferation of demand response (DR), which can be implemented in smart cities to enable energy consumers to proactively adjust how and when to use (or produce) the energy in accordance with the cost (or the reward) [4]. Particularly, the integration of DR with Internet of EVs (IoEV), i.e., IoEV-based DR, provides a promising way to flatten out the peak load and reduce the level of volatility without deploying additional generators and storage devices [5]. The integration advantages can be summarized from two perspectives: the communication perspective and the energy perspective. On one hand, IoEV enables seamless information collection of vehicle conditions, driving behaviors, route trajectories, energy states, and road environment, which is of significant importance for realizing intelligent energy scheduling in smart cities [6]. On the other hand, an array of connected EVs can either be used as a responsive load to absorb the excessive energy, or be regarded as a backup energy source during the peak time. This new energy management paradigm will also spur an array of smart city-related applications such as energy local area networks, virtual power plant, etc., [5], [7]. It is noted that IoEV is a more general concept than vehicle to gird (V2G). Besides V2G, IoEV may contain and support a great variety of application scenarios including vehicle to home (V2H), vehicle to building (V2B), vehicle to community (V2C), and vehicle to vehicle (V2V) [8].

The studies on IoEV-based DR have received considerable attentions from both industry and academia. A distributed EV cooperation mechanism was proposed in [9], which not only enables the efficient management of charging and discharging operations, but also offers V2G regulation services to support grid operation. In [10], Yu *et al.* investigated the EV charging and discharging cooperation management problem and proposed a coalition game-based solution to provide EV owners with better satisfaction in terms of vehicle battery status and economic profits.

However, despite the above-mentioned works, the research and development in this field are still in its infancy. The city-wide deployment of IoEV-based DR confronts the following critical challenges.

Manuscript received May 15, 2018; revised August 5, 2018 and September 17, 2018; accepted October 14, 2018. Date of current version May 23, 2019. This work was supported in part by the National Science Foundation of China under Grant 61601181, by the Fundamental Research Funds for the Central Universities under Grant 2017MS001, by the Beijing Natural Science Foundation under Grant 4174104, and by the Beijing Outstanding Young Talent under Grant 2016000020124G081. *(Corresponding author: Yan Zhang.)*

Z. Zhou, B. Wang, and Y. Guo are with the State Key Laboratory of Alternate Electrical Power System with Renewable Energy Sources, School of Electrical and Electronic Engineering, North China Electric Power University, Beijing 102206, China (e-mail: zhenyu_zhou@ncepu.edu.cn; wbc0203@163.com; 13264243417@139.com).

Y. Zhang is with the Department of Informatics, University of Oslo, 0315 Oslo, Norway. He is also with Simula Research Laboratory 1364 Fornebu, Norway (e-mail: yanzhang@ieee.org).

Digital Object Identifier 10.1109/TETCI.2018.2880693

First, there lacks a secure energy trading mechanism. Conventional DR relies on a trusted third party to audit and verify every transaction of energy trading [11], which is vulnerable to a series of security threats such as single point of failure, denial of service attacks, and privacy leakage [12], [13]. For example, a transaction record may be changed, tampered, or deleted by some malicious middleman attackers. However, most of the current works mainly concentrate on charging and discharging management in IoEV [5], [9], [10], [14], while the security and privacy issues which are significant to facilitate energy trading are not considered. Therefore, a secure energy trading mechanism is indispensable to guarantee the reliable operation of IoEV-based DR in an untrusted and nontransparent energy market.

Second, there lacks an incentive-compatible DR mechanism. Due to the increased battery consumption and other costs incurred by discharging, EV owners are reluctant to participate in large-scale decentralized energy trading unless they are well compensated [15], [16]. For example, a major impediment of EV discharging is the range anxiety, i.e., the fear of being stranded by a depleted battery due to the limited cruising range and the long charging time [17]. Hence, when designing the DR mechanism, the impact of the range anxiety has to be considered, and a sufficient amount of energy must be preserved for EV owners in order to reach their destinations.

EVs can be classified into different types based on their preferences towards DR participation. The EV type depends on numerous parameters including the state of charge (SoC) of the battery, the traveling schedule, the battery capacity, etc., and may vary significantly. Intuitively, EVs with higher types are prone to participate in energy trading and contribute more energy. For example, EVs with larger discharging capabilities can generate more energy during the peak time to bridge the gap between local supply and demand. Therefore, a well-designed DR mechanism should motivate EVs with higher types to participate in peak-time discharging. However, the type of each EV is private information, which is only known by the EV itself. That is, the information is asymmetric. Most of the previous works, e.g., [5], [9], [10], [18], [19] assume that the EV type is perfectly known, and cannot be applied to DR with asymmetric information. Therefore, it is of vital importance to develop an incentive-compatible DR mechanism, which can effectively optimize the economic performance under the information asymmetry scenario.

Accordingly, these challenges motivate us to develop a new DR framework for IoEV, which leverages blockchain, contract theoretical modeling, and computational intelligence to provide secure and efficient energy trading. Blockchain, in which every transaction is recorded in a verifiable and permanent way, has demonstrated its potential to secure energy trading due to the advantages of security, decentralization, and trust [11]. Recent works have explored blockchain to address the transaction security issues of energy trading in IoEV. Liu *et al.* proposed a decentralized blockchain-enabled EV charging scheme to simultaneously minimize the fluctuation level of the power grid and the EV charging cost [20]. In [21], Li *et al.* proposed a blockchain-based peer-to-peer energy trading system for industrial Internet of things, which relies on a credit-based payment strategy to reduce transaction confirmation latency. [22] However, due to the high computation cost associated with solving proof-of-work puzzles, blockchain has not been widely deployed in EVs with limited computing capabilities. Therefore, we adopt the consortium blockchain [23], in which a distributed ledger is created, publicly audited, and shared by multiple authorized nodes with moderate cost.

Furthermore, we put forward a contract theory-based incentive mechanism to maximize the social welfare. Contract theory provides a powerful tool for addressing the incentive problem with information asymmetry [24], and has already been widely applied in various applications including device-to-device communications [25], cognitive radio [24], and small-cell caching systems [26]. In most of previous contract theory related works, the probability distribution of each type is assumed as a priori information. However, this assumption may be too optimistic in practical implementation. Different from previous works, we provide a computational intelligence technique to derive the probability distribution of each type. Specifically, we demonstrate that the EV type depends on the SoC, which can be estimated by utilizing a machine learning-based approach.

Numerous SoC estimation methods have been proposed [27]. One category of SoC estimation methods has been developed based on the physical circuit models, including open-circuit voltage measurement [28], Columb counting [29], Kalman filters [30], etc. Another line of works rely on the emerging computational intelligence techniques, e.g., machine learning, which do not require the precise physical model of battery and circuit. Several computational intelligence-based SoC estimation methods have been proposed, such as neural network [31], support vector machine [32], and Gaussian process regression (GPR) [27]. In this work, we adopt the GPR scheme to obtain the probability distribution of the SoC based on current, voltage, and temperature measurements. The GPR-based SoC estimation has already been intensively investigated in a number of previous works [27], [33], [34].

B. Contributions

To the best of the authors' knowledge, this is the first work which provides a secure and efficient energy trading framework for IoEV-based DR by combining consortium blockchain, contract theoretical modeling, and computational intelligence. The contributions of this work are summarized as follows:

- *Consortium blockchain for secure energy trading:* We develop a consortium blockchain-enabled secure energy trading mechanism. All the transactions are created, propagated, and verified by authorized local energy aggregators (LEAGs) with moderate cost. The privacy and security properties are also analyzed.
- *Contract-based incentive-compatible DR mechanism:* We propose an incentive-compatible DR mechanism based on contract theoretical modeling. The contract is tailored for the unique characteristics of each EV type to maximize the social welfare under the constraints of individual rationality (IR), incentive compatibility (IC), and monotonicity.
- *Optimal contract design with/without information asymmetry:* The formulated social welfare maximization

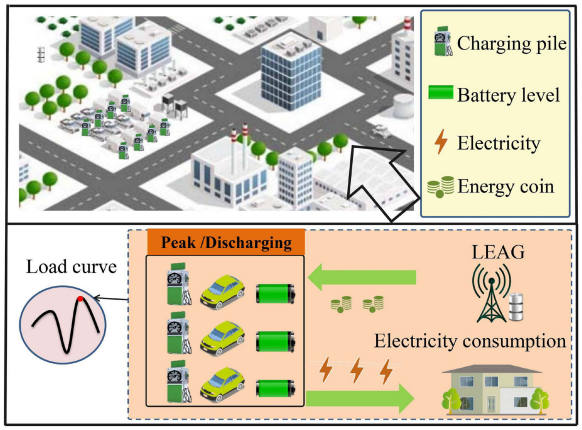

Fig. 1. A scenario of DR in IoEV.

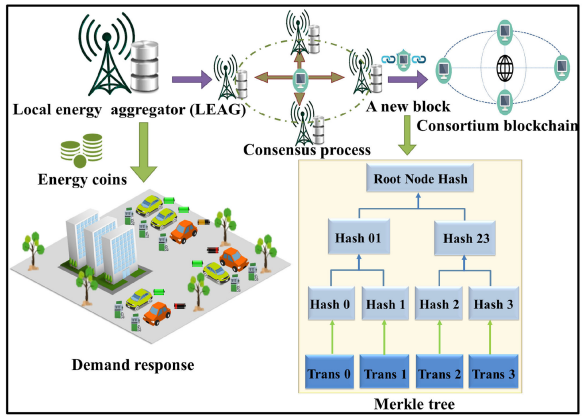

Fig. 2. Consortium blockchain-based secure energy trading.

problem falls into the category of difference of convex (DC) programming. To provide a tractable solution, we reduce the total number of IR and IC constraints by exploring the relationships between adjacent EV types. Then, the simplified problem is solved by using the iterative convex-concave procedure (CCP) algorithm. We also develop the contract without information asymmetry and the take-it-or-leave contract as performance benchmarks.

- *Computational intelligence-enabled SoC estimation:* We show how to derive the probability distribution of the EV type by exploring computational intelligence based SoC estimation techniques. Specifically, a GPR-based estimation scheme is adopted, and the corresponding offline training and the online estimation stages are elaborated in details.
- *Theoretical analysis and performance validation:* We provide a comprehensive theoretical analysis on contract feasibility, convergence, and energy trading security. The relationships among social welfare, EV type, reward, discharged electricity, and SoC estimation error are also elaborated via numerical results.

The remainder of this paper is organized as follows. Section II introduces the principle of the consortium blockchain-based secure energy trading. Section III presents the contract-based incentive-compatible DR mechanism for IoEV. Section IV illustrates the computational intelligence-enabled SoC estimation. Section V presents the analysis and comparison of computational complexity. Section VI shows the simulation results. Finally, Section VII concludes this paper.

II. Consortium Blockchain-based Secure Energy Trading

A. System Model

A typical scenario of DR in IoEV is shown in Fig. 1. There exist two major entities: EVs and LEAG. With bi-directional energy trading becoming feasible, any EV can either act as a responsive load or as an energy source. Particularly, each EV can actively adjust its charging and discharging behaviors based on the properly designed incentive mechanism. The LEAG provides energy trading related services including real-time data collection, 24/7 continuous status monitoring, and charging/discharging coordination. For the sake of simplicity, only the discharging management is considered here. During the peak time, the LEAG employs a set of discharging EVs to meet the demand locally. Meanwhile, the involved discharging EVs will obtain dedicated payments for their contributions to local supply-demand balance. Here, energy coin which is one kind of digital cryptocurrency is employed to facilitate the energy trading. The details for how to design the incentive mechanism will be illustrated in Subsection III-B.

There are three major components in the LEAG: a memory server, an account server, and a transaction server. All of the transaction records in the consortium blockchain are stored in the memory server. The digital assets of each EV in terms of energy coins are stored in a digital wallet. To preserve privacy, the true address of the wallet is replaced by a set of public keys, e.g., random pseudonyms. Each EV also has a transaction account which stores all of its transaction records. The mapping relationships between random wallet addresses and the corresponding transaction account are maintained in the account server. The transaction server is responsible to design incentive mechanisms and coordinate charging and discharging activities.

B. Implementation

The operation details of the consortium blockchain-based energy trading are shown in Fig. 2. In system initialization, existing cryptographic algorithms such as elliptic curve digital signature, Boneh-Boyen short signature, and SHA-256, can be utilized. An EV has to register with a legitimate authority to obtain its public key, privacy key, and certificate. For example, EVs with larger discharging capabilities can discharge more energy during the peak time to bridge the gap between local supply and demand. The certificate represents a unique identity for the EV via binding its registration information. Each EV has a set of wallet addresses issued by the authority. During system initialization, each EV finds the wallet address that is used by its nearest LEAG, verifies the wallet integrity, and downloads the corresponding data from the memory server.

The LEAG designs a contract, which specifies the relationship between the performance, i.e., the amount of energy required from a discharging EV, and the reward, i.e., the payment for

the discharging EV in terms of energy coins. In the contract, each distinct performance-reward association is defined as a contract item, and a contract generally contains a great variety of contract items. Then, the LEAG broadcasts the contract, and each EV chooses its desired contract item to maximize its payoff. After energy trading, a discharging EV will receive the specified reward if the corresponding contract item has been successfully fulfilled. The energy coins are transferred from the LEAG to the wallet address of the EV. The authenticity of the payment can be verified by checking the last block of the consortium blockchain. The LEAG sets up a new transaction record which has to be firstly verified and digitally signed by the EV, and then uploaded for public audit.

All of the transaction records collected by a LEAG within a certain period will be encrypted, digitally signed, and then structured into blocks. Invalid transactions, e.g., fake transactions, will be discarded. Each new block is linked to the prior block in the consortium blockchain by a cryptographic hash. Then, similar to the proof-of-work process in Bitcoin, each authorized LEAG in the consortium blockchain competes to create a block by finding a valid proof-of-work, i.e., a hash value which satisfies certain difficulty requirement. The hash value is calculated based on a random nonce value α, and a data set Φ which includes the hash value of the prior block, timestamp, and other necessary data. A valid α must satisfy $\text{Hash}(\alpha + \Phi) < \beta$, where β represents the level of difficulty.

The LEAG which is the first to find a valid proof-of-work broadcasts the created block to all of the authorized LEAGs in the network. Next, each LEAG audits and verifies the transaction records in the received block, and chooses whether to accept this new block or not. If a new block is accepted by all the LEAGs, i.e., a consensus has been reached, then it will be appended at the end of the current consortium blockchain, and the LEAG which created this block will be rewarded by a certain amount of energy coins.

III. Contract-based Incentive-Compatible Demand Response for Internet of Electric Vehicles

A. EV Type Modeling

We use EV type to quantify the preference of an EV towards discharging, which is only known by the EV itself. A higher-type EV is more willing to participate in the DR and discharge a larger amount of electricity to gain a higher reward. It is intuitive that EVs with higher types are more preferred by the LEAG. For the sake of simplicity, we assume that the set of EV types belongs to a discrete and finite space. The EV type is defined as follows.

Definition 1: Considering a parking lot with K discharging EVs, these EVs can be sorted in an ascending order based on their preferences and classified into K types. If the set of EV types is denoted as $\Theta = \{\theta_1, \ldots, \theta_k, \ldots, \theta_K\}$, then we have

$$\theta_1 < \cdots < \theta_k < \cdots < \theta_K, \quad k = 1, \ldots, K. \tag{1}$$

In the following, we derive the specific expression of the EV type. SoC, which is defined as the ratio of the currently available energy to the total battery capacity [35], is used as a benchmark to measure the battery condition. Considering type θ_k EV, the corresponding SoC is calculated as

$$SoC_k^c = \frac{E_k^c}{E_{k,\max}}, \tag{2}$$

where E_k^c represents the amount of currently available energy, and $E_{k,\max}$ is the battery capacity. After discharging, the remaining SoC should satisfy the minimum energy requirement of traveling, which is given by

$$\frac{E_k^c - L_k}{E_{k,\max}} \geq \chi(d_k), \tag{3}$$

where L_k is the required amount of electricity, and d_k is the distance that has to be traveled before the next charging. $\chi(d_k)$ denotes required electricity to travel the distance d_k, which is a monotonically increasing function of d_k. By combining (2) and (3), we can derive the discharging capability, which is given by

$$L_k \leq [SoC_k^c - \chi(d_k)]E_{k,\max}. \tag{4}$$

Hence, type θ_k can be defined as

$$\theta_k = [SoC_k^c - \chi(d_k)]E_{k,\max}. \tag{5}$$

Remark 1: From (5), it is observed that θ_k is positively proportional to SoC_k^c and $E_{k,\max}$, and inversely proportional to $\chi(d_k)$. For example, a larger EV type represents that either the EV has more energy available, or it will not travel a long distance in the near future.

In the information asymmetry scenario, the LEAG does not know the specific type of each EV, but only has the knowledge of the probability distribution of each type. We assume that the LEAG knows that there are a total of K types of discharging EVs and the specific probability that an EV belongs to type $\theta_k, \forall \theta_k \in \Theta$. We use the expression $P_{k',k}$ to denote the probability that EV k', i.e., $k' = 1, 2, \ldots, K$, belongs to type θ_k. Thus, we have $\sum_{k=1}^{K} P_{k',k} = 1$. $P_{k',k}$ can be obtained based on historical observation data. How to estimate P_k for practical implementation is provided in Section IV. For the sake of simplicity, we assume that the type probabilities of all the EVs follow an identical distribution, i.e., $P_{k',k} = P_{k'',k}$ $(k' \neq k'')$. In this way, the first subscript can be removed, and $P_{k',k}$ is simplified as P_k. Nevertheless, the system model and the proposed algorithm can be simply extended to the case where the type probability of each EV follows a different distribution.

B. Contract Formulation

Instead of providing the same contract for EVs with different types, a contract which consists of K contract items is designed for K types of discharging EVs, i.e., one for each type. For example, the contract item designed for type θ_k EV is denoted as (L_k, R_k), where L_k denotes the required electricity, and R_k is the dedicated reward in terms of energy coins. The contract is defined as $\mathcal{C} = \{(L_k, R_k), \forall k \in \mathcal{K}\}$, where $\mathcal{K} = \{1, \ldots, k, \ldots, K\}$.

Considering the K types of EVs, the expected utility of the LEAG is the sum of the revenue for all discharged electricity

minus all the reward, which can be calculated as

$$U_L(\{L_k\},\{R_k\}) = K\sum_{k=1}^{K} P_k(\gamma_L L_k - R_k), \tag{6}$$

where γ_L is the unit value of electricity for the LEAG.

Remark 2: A contract item $(L_k = 0, R_k = 0)$ means that type θ_k EV does not intend to participate in discharging. On the other hand, for EV discharging to be beneficial for the LEAG, the inequality $\gamma_L L_k - R_k \geq 0$ must hold. Otherwise, the LEAG has no incentive to employ type θ_k EV for discharging.

The utility function of type θ_k EV which accepts the contract item (L_k, R_k) is the reward offered minus the cost of discharged electricity, given by

$$U_k^{EV}(L_k, R_k) = \theta_k m(R_k) - \gamma L_k, \tag{7}$$

where γ is the unit cost of discharging the battery. $\theta_k m(R_k)$ represents the v alue of R_k for type θ_k EV. The function $m(R_k)$ is a monotonically increasing concave function of R_k, where $m(0) = 0$, $m'(R_k) > 0$, and $m''(R_k) < 0$. Without loss of generality, $m(R_k)$ can be defined as a quadratic function, i.e.,

$$m(R_k) = -\frac{a}{2}R_k^2 + bR_k, \tag{8}$$

where a and b are assumed as constants, which should satisfy $m'(R_k) > 0$ and $m''(R_k) < 0$. Nevertheless, the proposed scheme can be extended to other forms.

The expected social welfare is the total sum utility of the LEAG and the K EVs, which is given by

$$SW(\{L_k\},\{R_k\}) = U_L(\{L_k\},\{R_k\}) + K\sum_{k=1}^{K} P_k U_k^{EV}(L_k, R_k). \tag{9}$$

The social welfare maximization problem under asymmetric information is formulated as

$$\begin{aligned}
\mathbf{P1}: \max_{\{L_k\},\{R_k\}} \; & SW(\{L_k\},\{R_k\}),\\
\text{s.t.} \quad & C_1: \theta_k m(R_k) - \gamma L_k \geq 0, \quad (IR)\\
& C_2: \theta_k m(R_k) - \gamma L_k \geq \theta_k m(R_{k'}) - \gamma L_{k'}, \quad (IC)\\
& C_3: 0 \leq R_1 < \cdots < R_k < \cdots < R_K,\\
& C_4: L_k \leq \theta_k,\\
& \quad \forall k, k' \in \mathcal{K},
\end{aligned} \tag{10}$$

where C_1, C_2 and C_3 represent the IR, IC, and monotonicity constraints, respectively. C_4 represents the upper bound of L_k.

Definition 2: The IR, IC, and monotonicity constraints are defined as follows:

- *Individual rationality (IR) constraint:* Type θ_k EV, $\forall k \in \mathcal{K}$, will get a nonnegative payoff if it selects the contract item (L_k, R_k).
- *Incentive compatibility (IC) constraint:* The IC constraint ensures the *self-revealing* property of the contract. For instance, type θ_k EV, $\forall k \in \mathcal{K}$, will get the maximum payoff if and only if it selects the contract item (L_k, R_k) designed for its own type.
- *Monotonicity constraint:* The reward of type θ_k EV, $\forall k \in \mathcal{K}$, should be higher than that of type θ_{k-1} EV, and lower than that of type θ_{k+1} EV.

Based on the IR, IC, and monotonicity constraints, the following properties can be derived.

Lemma 1: For any $k, k' \in \mathcal{K}$, if $\theta_k > \theta_{k'}$, then $R_k > R_{k'}$. $R_k = R_{k'}$ if and only if $\theta_k = \theta_{k'}$.

Lemma 2: For any $L_k, R_k \in \mathcal{C}$, the following inequalities hold

$$\begin{aligned}
&0 \leq R_1 \leq \cdots \leq R_k \leq \cdots \leq R_K,\\
&0 \leq L_1 \leq \cdots \leq L_k \leq \cdots \leq L_K,\\
&0 \leq U_1^{EV} \leq \cdots \leq U_k^{EV} \leq \cdots \leq U_K^{EV}.
\end{aligned} \tag{11}$$

Proof: The detailed proof of Lemma 1 and Lemma 2 are omitted here due to space limitation. A similar proof can be found in [25]. ■

C. Optimal Contract Design under Information Asymmetry

1) Contract Feasibility: First, we define the sufficient and necessary conditions for contract feasibility.

Theorem 1: Contract feasibility: The contract $\mathcal{C} = \{(L_k, R_k), \forall k \in \mathcal{K}\}$ is feasible if and only if all the following conditions are satisfied:

- $0 \leq R_1 \leq \cdots \leq R_k \leq \cdots \leq R_K$ and $0 \leq L_1 \leq \cdots \leq L_k \leq \cdots \leq L_K$;
- $\theta_1 m(R_1) - \gamma L_1 \geq 0$;
- For any $k \in \{2, \ldots, K\}$, $\gamma L_{k-1} + \theta_{k-1}[m(R_k) - m(R_{k-1})] \leq \gamma L_k \leq \gamma L_{k-1} + \theta_k[m(R_k) - m(R_{k-1})]$.

Proof: The detailed proof of Theorem 1 is omitted here due to space limitation. A similar proof can be found in [24, Appendix D]. ■

2) Problem Transformation: The social welfare maximization problem **P1** involves K IR constraints and $K(K-1)$ IC constraints. To provide a tractable solution, the following procedures are carried out to simplify the problem.

Step 1: IR Constraints Elimination

For type θ_k EV, $k \in \mathcal{K}, k \neq 1$, we can derive

$$\theta_k m(R_k) - \gamma L_k \geq \theta_k m(R_1) - \gamma L_1 > \theta_1 m(R_1) - \gamma L_1 \geq 0, \tag{12}$$

where the first inequality is due to the IC constraint, the second equality is due to $\theta_k > \theta_1$, and the third inequality is due to the IR constraint. Hence, if the IR constraint of type θ_1 EV is guaranteed, then the IR constraints of EVs with higher types are automatically satisfied.

Step 2: IC Constraints Elimination

We define the IC constraints between type θ_k and type $\theta_{k'}$, $k' \in \{1, \ldots, k-1\}$, as downward incentive constraints (DICs). Similarly, the IC constraints between type θ_k and type $\theta_{k'}$, $k' \in \{k+1, \ldots, K\}$, are defined as upward incentive constraints (UICs). In the following, we show that both the DICs and UICs can be reduced.

We consider three adjacent EV types, i.e., $\theta_{k-1} < \theta_k < \theta_{k+1}$, which satisfy

$$\theta_{k+1} m(R_{k+1}) - \gamma L_{k+1} \geq \theta_{k+1} m(R_k) - \gamma L_k, \tag{13}$$

Algorithm 1: CCP Algorithm.

1: **Input:** $R_{k,0}[\tau]$, Θ, γ_L, γ.
2: **Output:** $\{\hat{L}_k\}, \{\hat{R}_k\}$
$\tau := 0$
3: **Repeat**
4: Transform the concave function $f_k(R_k), \forall k \in \mathcal{K}$, into an affine function by using (18).
5: Transform $\mathbf{P2}$ into a convex programming problem.
6: Obtain $\{\hat{L}_k[\tau]\}$ and $\{\hat{R}_k[\tau]\}$ by using KKT conditions.
7: Update. $\tau := \tau + 1$, $R_{k,0}[\tau+1] = \hat{R}_k[\tau], \forall k \in \mathcal{K}$.
Until satisfying the stopping criterion (21).

$$\theta_k m(R_k) - \gamma L_k \geq \theta_k m(R_{k-1}) - \gamma L_{k-1}, \tag{14}$$

where (13) denotes the DIC between type θ_{k+1} and type θ_k, and (14) denotes the DIC between type θ_k and θ_{k-1}.

By combining $R_{k+1} \geq R_k \geq R_{k-1}$, we have

$$\theta_{k+1} m(R_{k+1}) - \gamma L_{k+1} \geq \theta_{k+1} m(R_{k-1}) - \gamma L_{k-1}. \tag{15}$$

Therefore, if the DIC between type θ_{k+1} and θ_k holds, then the DIC between θ_{k+1} and θ_{k-1} also holds. The DIC constraints can be extended downward from type θ_{k-1} to type θ_1, which are given by

$$\begin{aligned} \theta_{k+1} m(R_{k+1}) - \gamma L_{k+1} &\geq \theta_{k+1} m(R_{k-1}) - \gamma L_{k-1}, \\ &\geq \cdots \\ &\geq \theta_{k+1} m(R_1) - \gamma L_1. \end{aligned} \tag{16}$$

Thus, we demonstrate that if the DICs between adjacent types hold, then all the DICs hold automatically. Similarly, we can demonstrate that if the UICs between adjacent types hold, then all the UICs hold automatically.

Based on the above analysis, the K IR constraints and $K(K-1)$ IC constraints can be reduced to 1 and $K-1$, respectively. $\mathbf{P1}$ is rewritten as

$$\begin{aligned} \mathbf{P2}: \max_{\{L_k\},\{R_k\}} \; & SW(\{L_k\},\{R_k\}), \\ \text{s.t.} \quad & C_1: \theta_1 m(R_1) - \gamma L_1 \geq 0, \quad (IR) \\ & C_2: \theta_k m(R_{k-1}) - \gamma L_{k-1} \leq \theta_k m(R_k) - \gamma L_k, \quad (IC) \\ & C_3, C_4, k = 2, \ldots, K. \end{aligned} \tag{17}$$

3) Optimal Contract with Reduced Constraints: We can prove that the objective of $\mathbf{P2}$ is a concave function by checking the Hessian matrix. However, convex programming cannot be directly applied here because the constraint C_2 involves the difference of two concave functions, i.e., $\theta_k m(R_{k-1}) - \gamma L_{k-1}$ and $\theta_k m(R_k) - \gamma L_k$. Therefore, the CCP algorithm proposed in [36] is adopted to solve $\mathbf{P2}$, which is summarized in Algorithm 1.

Denote $f_k(R_k) = \theta_k m(R_k)$. Since $f_k(R_k)$ is differentiable with regards to R_k, $f_k(R_k)$ can be approximated by using its first-order Taylor series expansion as

$$f_k(R_k) \approx f_k(R_{k,0}[\tau]) + \nabla f_k(R_{k,0}[\tau])(R_k - R_{k,0}[\tau]), \tag{18}$$

where $R_{k,0}[\tau]$ represents the initial point at iteration τ.

Hence, the constraint C_2 with the difference of two concave functions is transformed to the difference of a concave function and an affine function, which is written as

$$\begin{aligned} \tilde{C}_2: \theta_k m(R_{k-1}) - \gamma L_{k-1} & \\ \leq f_k(R_{k,0}[\tau]) + \nabla f_k(R_{k,0}[\tau])(R_k - R_{k,0}[\tau]). & \end{aligned} \tag{19, 20}$$

By replacing C_2 with $\tilde{C}_2$, $\mathbf{P2}$ is transformed into a convex programming problem, and can be easily solved by using Karush-Kuhn-Tucker (KKT) conditions. At each iteration τ, the local optimal solutions $\hat{L}_k[\tau]$ and $\hat{R}_k[\tau]$ are obtained by solving the transformed convex problem. Then, the initial point for Taylor series expansion at iteration $\tau+1$ is defined as $R_{k,0}[\tau+1] = \hat{R}_k[\tau]$. Next, the above iteration is repeated to derive a new local optimal solution.

The iterative process terminates until a predefined stopping criterion is satisfied. For example, the improvement in the social welfare is less than or equal to some positive threshold ϵ, i.e.,

$$\begin{aligned} SW\big(\{\hat{L}_k[\tau+1]\},\{\hat{R}_k[\tau+1]\}\big) - SW\big(\{\hat{L}_k[\tau]\},\{\hat{R}_k[\tau]\}\big) & \\ \leq \epsilon. & \end{aligned} \tag{21}$$

Theorem 2: Convergence: At any iteration τ, the obtained $\{\hat{L}_k[\tau]\}$ and $\{\hat{R}_k[\tau]\}$ are feasible. Furthermore, $\{SW\}_{\tau=0}^{\infty}$ is nondecreasing, and will converge to the maximum social welfare, i.e.,

$$SW\big(\{\hat{L}_k[\tau]\},\{\hat{R}_k[\tau]\}\big) \leq SW\big(\{\hat{L}_k[\tau+1]\},\{\hat{R}_k[\tau+1]\}\big). \tag{22}$$

Proof: The detailed proof of Theorem 2 is omitted here. A similar proof can be found in [36]. ■

D. Optimal Contract Design Without Information Asymmetry

If there exists a selfish LEAG which is precisely aware of each EV's type, it can further increase its profit as long as each EV only accepts the contract item designed for its own type. In this scenario, the LEAG has to ensure that the payoff of each EV is non-negative, otherwise, the EVs have no incentive to accept the contract item. To this end, the contract item has to meet the IR constraint. Furthermore, the contract item has to satisfy the following property:

Proposition 1: In the contract design without information asymmetry, any contract item $(L_k, R_k) \in \mathcal{C}$ should satisfy $\theta_k m(R_k) = \gamma L_K$. That is, the payoff for any EV is zero.

Proof: Proposition 1 can be proved by contradiction. Given an optimal contract item (R_k, L_k), if $\theta_k m(R_k) - \gamma L_k > 0$, then the LEAG can increase its utility by increasing L_k until $\theta_k m(R_k) - \gamma L_k = 0$. This contradicts with the assumption that (L_k, R_k) is optimal. ■

Thus, by enforcing the utility of each EV to be zero, the social welfare is equivalent to the utility of the LEAG. The corresponding optimization problem is formulated as

$$\begin{aligned} \mathbf{P3}: \max_{\{L_k\},\{R_k\}} \; & SW(\{L_k\},\{R_k\}), \\ \text{s.t.} \quad & C_1: \theta_k m(R_k) - \gamma L_k = 0, \\ & C_2: 0 \leq R_1 < \cdots < R_k < \cdots < R_K, \\ & C_3, C_4, \forall k \in \mathcal{K}. \end{aligned} \tag{23}$$

To solve (23), we have to work out the solutions of K quadratic equations, i.e., $\theta_k m(R_k) - \gamma L_k = 0$, $\forall k \in \mathcal{K}$. Assuming that R_{k1} and R_{k2} are the two solutions of the k-th quadratic equation, the optimal solution is given by

$$(\{L_k\}, \{R_k\}) = \underset{\{R_k\} \in (\{R_{k1}\}, \{R_{k2}\})}{\arg\max} (SW(\{L_{k1}\}, \{R_{k1}\}), SW(\{L_{k2}\}, \{R_{k2}\})) \tag{24}$$

Proposition 2: In the contract design without information asymmetry, for any EV type θ_k, $k \in \mathcal{K}$, R_k is fixed regardless of θ_k.

Proof: Substituting $\theta_k m(R_k) - \gamma L_k = 0$ into (9), it can be verified that the social welfare SW increases monotonically with $\sum_{k=1}^{K} L_k$. Hence, the LEAG can increase L_k until $L_k = \theta_k$. Next, substituting $L_k = \theta_k$ into $\theta_k m(R_k) - \gamma L_k = 0$, we have $m(R_k) = \gamma_L$, which means R_k is fixed regardless of θ_k. ■

IV. Computational Intelligence-Based SoC Estimation

In practical implementation, there exists an extreme scenario that neither the precise information nor the probability distribution of EV type is known by the LEAG. This scenario has been largely ignored by most of previous studies. In this work, we investigate how to predict the probability distribution of EV type by exploring computational intelligence techniques.

By observing (5), an EV type θ_k, $\forall k \in \mathcal{K}$, depends on SoC SoC_k^c, future travel distance d_k, and battery capacity $E_{k,\max}$. Among these three parameters, the future travel distance d_k depends on the moving habits of EV owners, and can be learnt from long-term history trajectories [37], while the battery capacity of each EV can be considered as a deterministic value during the optimization process. Thus, the EV type merely depends on the SoC. However, it is difficult to directly measure the value of SoC because the energy is stored in a chemical form, and a battery system exhibits highly nonlinear features.

We adopt the GPR-based SoC estimation method, which contains two stages: the offline training stage and the online estimation stage. A brief introduction is provided as follows. Interested readers can refer to [27] and [38] for more details.

In the offline training stage, a D-dimensional training data set $\mathcal{D} = (\mathbf{X}, \mathbf{SoC})$ is utilized to train the GPR estimator to learn the relationship between voltage, current, temperature, and SoC. $\mathbf{X}$ contains N input vectors, i.e., $\mathbf{X} = \{\mathbf{x}_1, \ldots, \mathbf{x}_n, \ldots, \mathbf{x}_N\}$, $\mathbf{x}_n \in \mathbf{R}^D$, which includes the voltage, current, and temperature measurements. $\mathbf{SoC}$ contains the corresponding normalized values of SoC, i.e., $\mathbf{SoC} = \{SoC_1, \ldots, SoC_n, \ldots, SoC_N\}$, $SoC_n \in \mathbf{R}$. The relationship between $\mathbf{X}$ and $\mathbf{SoC}$ is characterized as

$$SoC_n = g(\mathbf{x}_n) + \varepsilon_n, \tag{25}$$

where ε_n represents an additive Gaussian noise with zero mean and variance σ_n^2, i.e., $\varepsilon_n \sim \mathcal{N}(0, \sigma_n^2)$. $g(\cdot)$ denotes the mapping from $\mathbf{X}$ to $\mathbf{SoC}$, which is unknown.

In GPR, it is assumed that the set of function values $\mathbf{g} = [g(\mathbf{x}_1), g(\mathbf{x}_2), \ldots g(\mathbf{x}_n)]^T$ follows a multivariate Gaussian distribution [38], i.e.,

$$P(\mathbf{g} \mid \mathbf{x}_1, \mathbf{x}_2, \cdots, \mathbf{x}_n) = \mathcal{N}(\mathbf{0}, \Lambda), \tag{26}$$

where $\mathbf{0}$ is an $N \times 1$ zero vector, and Λ is a kernel matrix, whose element $\Lambda_{ij} = \lambda_s(\mathbf{x}_i, \mathbf{x}_j)$ represents the value of the kernel function. The kernel function specifies the inner product of two vectors in feature space. Here, we use the automatic relevance determination (ARD) squared exponential kernel function, and $\lambda(\mathbf{x}_i, \mathbf{x}_j)$ can be determined as

$$\lambda_s(\mathbf{x}_i, \mathbf{x}_j) = \zeta_0^2 \exp\left[-\frac{1}{2}\sum_{d=1}^{D}\left(\frac{x_{id} - x_{jd}}{l_d}\right)^2\right], \tag{27}$$

where x_{id} and x_{jd} correspond to the d-th element of vectors $\mathbf{x}_i$ and $\mathbf{x}_j$, respectively. ζ_0^2 denotes the variation of $\mathbf{g}$ from its mean, and l_d denotes the relative importance of each input variable in estimating the target output.

In the case of noisy observation, the kernel function with additive noise is defined as

$$\lambda(\mathbf{x}_i, \mathbf{x}_j) = \lambda_s(\mathbf{x}_i, \mathbf{x}_j) + \sigma_n^2 \delta_{ij}. \tag{28}$$

More detailed definitions and explanations can be found in [27] and [38].

Then, the distribution of $\mathbf{SoC}$ is given by

$$\begin{aligned} P(\mathbf{SoC} \mid \mathbf{X}) &= \int P(\mathbf{SoC} \mid \mathbf{g}, \mathbf{X}) P(\mathbf{g} \mid \mathbf{X}) d\mathbf{g} \\ &= \mathcal{N}\left(\mathbf{0}, \mathbf{\Lambda} + \sigma_n^2 \mathbf{I}\right). \end{aligned} \tag{29}$$

where $\mathbf{I}$ is an $N \times N$ identity matrix. Then, the marginal log-likelihood of $\mathbf{SoC}$ can be written as

$$\begin{aligned} \log P(\mathbf{SoC} \,|\mathbf{X}, \mathbf{h}) = &-\frac{1}{2}\mathbf{SoC}^T (\mathbf{\Lambda} + \sigma_n^2 \mathbf{I})^{-1} \mathbf{SoC} \\ &- \frac{1}{2}\log\left|\mathbf{\Lambda} + \sigma_n^2 \mathbf{I}\right| - \frac{N}{2}\log 2\pi. \end{aligned} \tag{30}$$

where $|.|$ denotes the determinant of a matrix.

Let $\mathbf{h} = [\zeta_0, l_1, \ldots, l_D]^T$ denote set of hyperparameters. The optimal hyperparameters which maximize the marginal log-likelihood function are calculated as

$$\begin{aligned} &\frac{\partial \log P(\mathbf{SoC} \,|\mathbf{X}, \mathbf{h})}{\partial \mathbf{h}_i} \\ &= -\frac{1}{2} tr\left(\left(\mathbf{\Lambda} + \sigma_n^2 \mathbf{I}\right)^{-1} \frac{\partial\left(\mathbf{\Lambda} + \sigma_n^2 \mathbf{I}\right)}{\partial \mathbf{h}_i}\right) \\ &\quad + \frac{1}{2}\mathbf{SoC}^T \left(\mathbf{\Lambda} + \sigma_n^2 \mathbf{I}\right)^{-1} \frac{\partial(\mathbf{\Lambda} + \sigma_n^2 \mathbf{I})}{\partial \mathbf{h}_i} \left(\mathbf{\Lambda} + \sigma_n^2 \mathbf{I}\right)^{-1} \mathbf{SoC}. \end{aligned} \tag{31}$$

Upon obtaining the optimal hyperparameters, the online estimation is performed to calculate the distribution of the test output $\widetilde{SoC}$ based on the dataset $\mathcal{D}$ and test input $\tilde{\mathbf{x}}$. Here, $\widetilde{SoC}$ is the SoC estimated based on $\mathbf{h}$, $\mathbf{X}$, $\mathbf{SoC}$, and $\tilde{\mathbf{x}}$. The joint distribution of the training outputs $\mathbf{SoC}$ and the test output $\widetilde{SoC}$

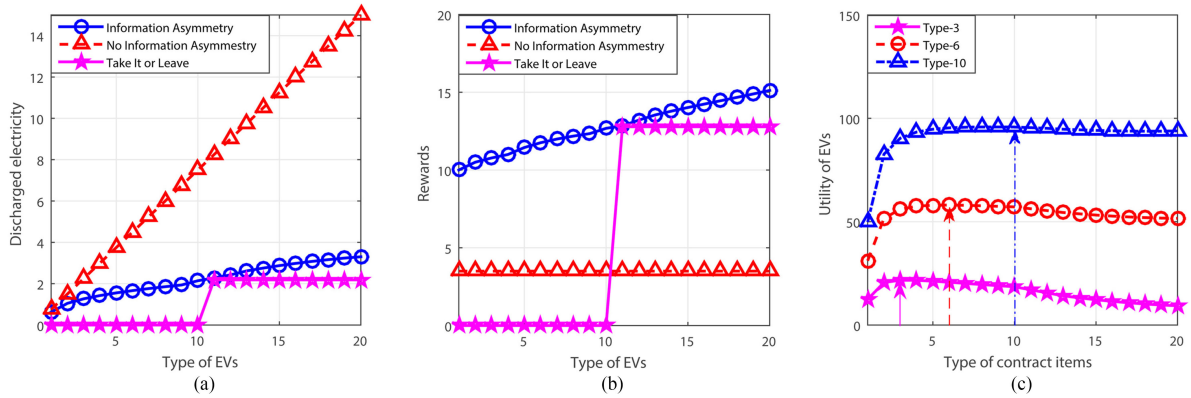

Fig. 3. Contract feasibility: (a) discharged electricity; (b) reward; (c) EV's utility.

is calculated as

$$P\left(\mathbf{SoC}, \widetilde{SoC} \middle| \mathbf{X}, \tilde{\mathbf{x}}, \mathbf{h}\right) = N\left(\begin{bmatrix}\mathbf{0}\\ 0\end{bmatrix}, \begin{bmatrix}\mathbf{\Lambda} + \sigma_n^2\mathbf{I} & \boldsymbol{\lambda}_*\\ \boldsymbol{\lambda}_*^T & \lambda_{**} + \sigma_n^2\end{bmatrix}\right). \quad (32)$$

By marginalizing $\log P(\mathbf{SoC}\,|\mathbf{X}, \mathbf{h})$ over the distribution of $\mathbf{SoC}$, the probability distribution of $\widetilde{SoC}$ is Gaussian, i.e.,

$$P\left(\widetilde{SoC} \mid \mathbf{X}, \mathbf{SoC}, \tilde{\mathbf{x}}, \Lambda\right) = \mathcal{N}(\mu_*, \Sigma_*), \quad (33)$$

where the mean and the covariance of the estimation distribution are given as follows:

$$\mu_* = \boldsymbol{\lambda}_*^T(\mathbf{\Lambda} + \sigma_n^2\mathbf{I})^{-1}\mathbf{SoC}, \quad (34)$$

$$\Sigma_* = \sigma_n^2 + \lambda_{**} - \boldsymbol{\lambda}_*^T(\mathbf{\Lambda} + \sigma_n^2\mathbf{I})^{-1}\boldsymbol{\lambda}_*. \quad (35)$$

V. Computational Complexity Analysis

Since there are K pairs of optimization variables, the overall computational complexity of constraint transformation is $O(K)$. After constraint transformation, for each EV type θ_k, the computational complexity to solve $\mathbf{P2}$ is $O(K)$. Thus, the overall computational complexity of the proposed scheme is $O(K^2)$. If the statistical knowledge of the SoC is unknown, the GPR-based SoC estimation scheme with a computational complexity of $O(N^2)$ has to be used.

The optimal loan pricing algorithm proposed in [21] has a two-layer structure. The first layer is to optimize loan amount with a computational complexity of $O(K)$. The second layer is to optimize bank utility with a computational complexity of $O(K)$. Therefore, the overall computational complexity is $O(K^2)$. The adaptive blockchain-based EV participation (AdBEV) scheme proposed in [20] comprises a main loop to update the order book with a computational complexity of $O(K)$. In each round of the main loop, two minor loops are carried out to implement the best order strategy and the iceberg execution, each of which has a computational complexity of $O(K)$. Thus, the overall computational complexity is $O(2K^2)$.

It is clear that our scheme has similar computational complexity compared to the algorithms proposed in [20] and [21] when the statistical knowledge of the EV type is a prior information. However, different from our scheme, the algorithms proposed in [20] and [21] cannot be applied for the scenario where the statistical knowledge of the EV type is unknown.

VI. Simulation Results

To verify the efficiency of the contract-based incentive-compatible DR mechanism, we consider a parking lot with $K = 20$ discharging EVs and one LEAG. The type of discharging EV is assumed to follow a Gaussian distribution. The battery capacity of any EV is 24 kWh. The unit cost of discharging the battery for any EV is 10 cent/kWh, i.e., $\gamma = 10$, and the unit value of electricity for the LEAG is 13 cent/kWh, i.e., $\gamma_L = 13$. The proposed scheme is compared with the contract without information asymmetry studied in [25] and the take-it-or-leave contract proposed in [24]. The take-it-or-leave contract is a threshold-based contract, in which every EV is offered with a uniform contract item regardless of the EV type. The contract item is designed based on a particular threshold type, e.g., type $\theta_{k'} = 11$. Then, EVs whose types are lower than the threshold type ($\theta_k < \theta_{k'}$) will refuse to sign the contract. The reason is that these EVs with lower types are unable to meet the specified discharging requirement. In comparison, EVs whose types are no less than the threshold type ($\theta_k \geq \theta_{k'}$) will sign the contract.

To evaluate the performance of SoC estimation, a total of 4×10^3 samples (including voltage, current, and temperature samples) are generated for each EV type based on the battery circuit model proposed in [27]. The first half of the generated samples are utilized as the training data to derive the optimal hyperparameters, while the remaining half are utilized as the testing data to verify the estimation performance. The root-mean-square error (RMSE) [39], which is defined as the square root of the second sample moment of the differences between the SoC values predicted by the GPR-based estimation scheme and the real SoC values, is adopted as the performance metric. It can be expressed as

$$RMSE = \sqrt{\frac{1}{n}\sum\nolimits_{n=1}^{N}\left(SoC_n - \widetilde{SoC}_n\right)^2}, \quad (36)$$

where $\widetilde{SoC}_n$ is the estimated value of SoC and SoC_n is the actual value of SoC.

Fig. 3(a) and Fig. 3(b) show the discharged electricity L_k and the reward R_k versus the EV type θ_k, respectively.

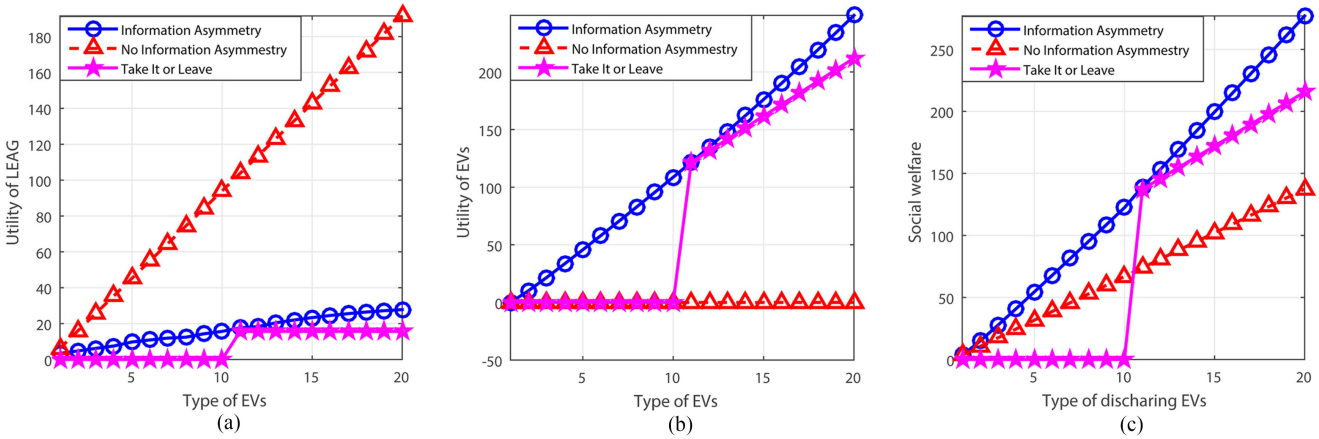

Fig. 4. System performance: (a) LEAG's utility; (b) EV's utility; (c) social welfare.

Numerical results show that the discharged electricity and the reward increase monotonically with the EV type, which is consistent with Lemma 2. Furthermore, it is observed that the contract without information asymmetry requires much higher amount of electricity from EVs compared to the contract with information asymmetry and take-it-or-leave contract, and provides every EV with the same reward. The reason behind has been demonstrated in Proposition 2. In the take-it-or-leave contract, only EVs whose types are no less than $\theta_{k'}$ will have nonzero discharged electricity and reward values, because the contract is designed for EVs whose types are no less than the threshold type $\theta_{k'}$.

Fig. 3(c) shows the utilities of type 3, type 6, and type 10 EVs versus the different types of contract items. Simulation results demonstrate that the proposed contract is incentive compatible. The maximum utility of each EV can be achieved if and only if the type of the selected contract item is consistent with the EV type. The utility of an EV degrades if it selects a contract item designed for EVs with different types. Furthermore, we can observe that the EV with higher type will also achieve a larger utility compared to that of lower type, which is consistent with Lemma 3.

Fig. 4(a) and Fig. 4(b) show the utility of the LEAG, e.g., U_L, and the utility of EV, e.g., U_k^{EV}, versus the EV type θ_k. Without information asymmetry, the LEAG can achieve a much higher utility, while the utility of any EV remains zero. The reason has been explained in the proof of Proposition 1. Thus, the EVs' utilities are much worse than those of the information asymmetry scenario. In other words, EVs can actually benefit from the presence of information asymmetry because the LEAG cannot extract all the available electricity from an EV without knowing the precise knowledge of its type. For the take-it-or-leave contract, the utilities of EVs and LEAG are zero when EV types are less than $\theta_{k'}$, which agrees with the results in Fig. 3(a) and Fig. 3(b).

Fig. 4(c) shows the social welfare SW versus the EV type θ_k. Numerical results show that the maximal social welfare achieved under the scenario of information asymmetry outperforms the performance without information asymmetry. The reason is that the utility gain of the LEAG cannot compensate the corresponding utility loss of EVs.

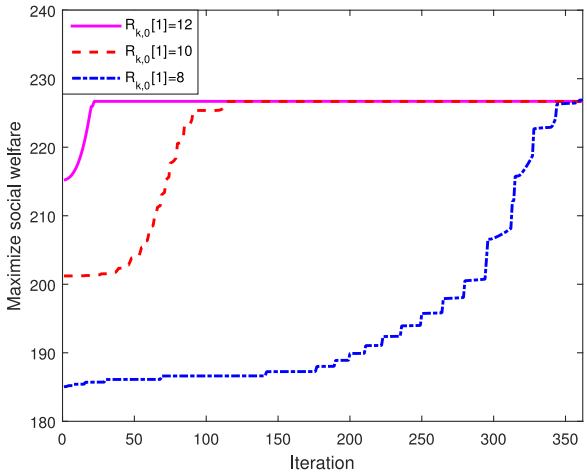

Fig. 5. The convergence performance of the proposed CCP-based solution.

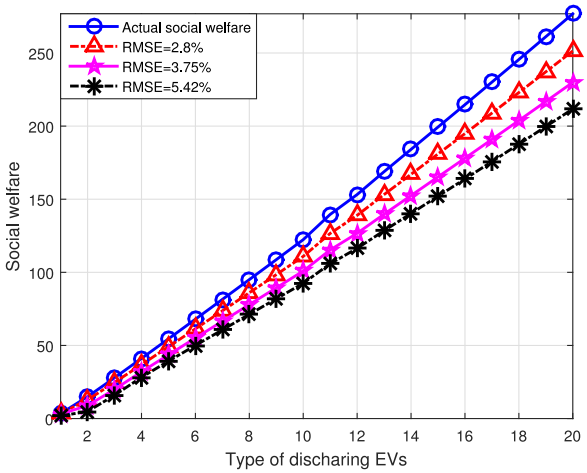

Fig. 6. The impact of estimation errors on the social welfare.

In the take-it-or-leave contract, only EVs whose types are no less than $\theta_{k'}$ will have nonzero utilities. The utility gap between the proposed scheme and the take-it-or-leave contract increases monotonically with the EV type. The reason is that the take-it-or-leave contract does not take into account the type varieties of different EVs. As a result, the performance gap between the

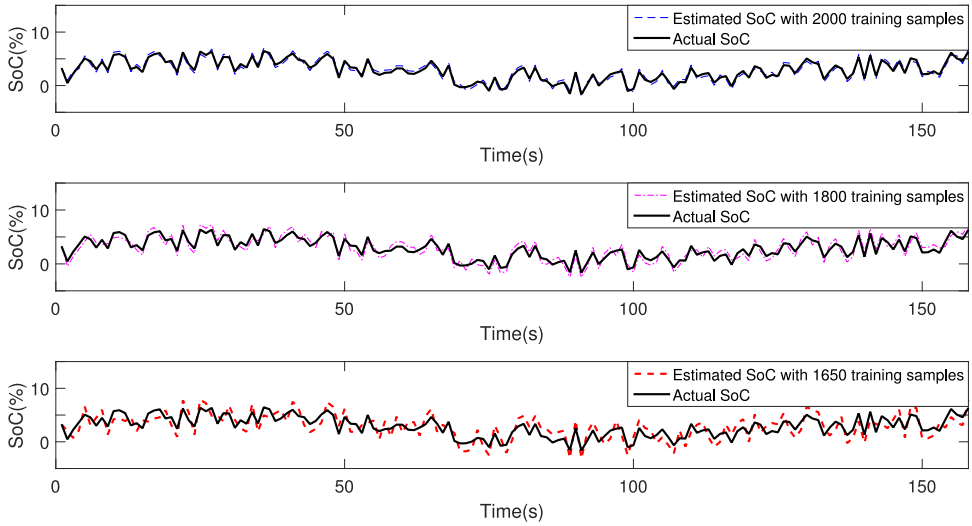

Fig. 7. SoC estimates versus training sample size.

proposed contract and the take-it-or-leave contract increases as the EV type deviates from the threshold type.

Fig. 5 shows the convergence performance of the proposed CCP-based solution. Three initial points, i.e., $\{R_{k,0}[1]\} = 8$, 10, and 12 are chosen to characterize the impact of initial point on the convergence speed. As the iteration number increases, all the three cases converge to the optimal social welfare within finite iterations. Particularly, the case with $\{R_{k,0}[1]\} = 12$ only requires 25 iterations to reach convergence. The reason is that 12 is closest to the average value of the optimal rewards shown in Fig. 3(b) (which is 12.774). In comparison, the case with $\{R_{k,0}[1]\} = 8$ requires more than 300 iterations. Thus, the position of the initial point plays an important role in algorithm convergence performance.

Fig. 6 shows the impact of estimation errors on the social welfare. The maximum achievable social welfare decreases as the RMSE increases. The reason is that a larger RMSE is more likely to result in an inaccurate estimation of the EV type, and the designed contract no longer satisfies the contract feasibility condition. For example, the LEAG may mistakenly regard type θ_k as type θ_{k+1}, and the derived contract item may violates the IR constraint, or the upper bound constraint $L_k \leq \theta_k$. Furthermore, the EV may also select the contract designed for EVs with different types and the corresponding utility is significantly lowered.

Fig. 7 shows the SoC estimates versus the training sample size. It is observed that the estimated SoC gets closer to the actual SoC as the training sample size increases. The reason is that more training samples provide additional information for improving the estimation accuracy. Hence, 2×10^3 training samples are sufficient to achieve an accurate estimation. It is important to maintain a good balance between the estimation accuracy and the training sample size.

The privacy and security properties are summarized as follows:

- Anonymity: Instead of using its true identity, each EV uses a unique public key to communicate with others, which prevents malicious attackers from tracking an EV's identity. Furthermore, an EV can change its public key after each transaction to avoid the linking attack, i.e., the different pieces of data belonging to the same EV are linked together to deanonymize the EV.
- Authentication: In the process of proof-of-work, every transaction has to be publicly audited and authenticated by authorized LEAGs. It is impossible to compromise all of the authorized LEAGs in the network.
- Integrity: Once a block has been appended into the blockchain, it contains the hash of the previous block, and its own hash will be contained in the subsequent block. Therefore, it is infeasible to modify the block unless the majority of the computing power are controlled by a malicious attacker. Moreover, the transaction data contained in a block are encrypted with asymmetric encryption techniques. It takes a tremendous cost to decrypt the encrypted data without knowing the private key.
- Transparency: Since the blockchain technology is open source, any user, software developer, and service provider can have access to the blockchain and monitor the corresponding transaction data. That is, the transaction data are not saved in one single node and are transparent to all entities. As a result, any malicious data modification can be noticeable and traceable.

VII. Conclusions

In this paper, we proposed a secure and efficient energy trading framework for IoEV-based DR by combining consortium blockchain, contract theoretical modeling, and computational intelligence. First, we proposed a consortium blockchain-based energy trading mechanism, which not only secures the energy trading by exploring its advantages of security, decentralization and trust, but also dramatically reduces computation cost. Then, a contract-based incentive-compatible DR mechanism was developed to maximize the social welfare under the scenario of information asymmetry. The social welfare maximization

problem was solved by using the iterative CCP algorithm. Next, we derived the probability distribution of the EV type by utilizing a GPR-based SoC estimation scheme based on voltage, current, and temperature data samples.

Numerical results demonstrate that the proposed scheme not only satisfies contract feasibility, but also yields good performance. The following conclusions are summarized: i) the proposed scheme is incentive compatible and outperforms other heuristic algorithms in terms of social welfare; ii) the presence of information asymmetric is beneficial to both EVs and the social welfare; iii) the position of initial points has a remarkable impact on the convergence performance; iv) that the accuracy of SoC estimation is proportional to the size of training sample and the social welfare value decreases as the RMSE increases.

A practical challenge that has been ignored in this work is that determining a block will cost a lot of computation resources, which prevents the blockchain-based energy trading from being widely deployed. To address such a challenge, one potential solution is to explore the edge computing-based task offloading approach [20], where the computation-intensive proof-of-work puzzles are processed by the powerful edge computing servers in the proximity of LEAGs to avoid unnecessary transmission and processing latency [40]. Future works will focus on how to integrate edge computing with blockchain to reduce the transaction confirmation latency, and how to develop a new DR framework for IoEV by considering the interactions among EVs, LEAGs, and edge computing service providers. Furthermore, the GPR-based SoC estimation method used in this work requires an offline training stage, which is still time consuming and maybe even unrealistic if the required training dataset is unavailable. To address such a challenge, an alternative approach is to explore unsupervised learning or reinforcement learning methods which do not require the offline training process. This will also be considered in our future work.

REFERENCES

[1] N. Kumar, A. V. Vasilakos, and J. J. P. C. Rodrigues, "A multi-tenant cloud-based DC nano grid for self-sustained smart buildings in smart cities," *IEEE Commun. Mag.*, vol. 55, no. 3, pp. 14–21, Mar. 2017.

[2] Z. Zhou *et al.*, "When mobile crowd sensing meets UAV: Energy-efficient task assignment and route planning," *IEEE Trans. Commun.*, vol. 66, no. 11, pp. 5526–5538, Nov. 2018.

[3] R. Yu, W. Zhong, S. Xie, C. Yuen, S. Gjessing, and Y. Zhang, "Balancing power demand through EV mobility in vehicle-to-grid mobile energy networks," *IEEE Trans. Ind. Inf.*, vol. 12, no. 1, pp. 79–90, Feb. 2016.

[4] A. H. Mohsenian-Rad, V. W. S. Wong, J. Jatskevich, R. Schober, and A. Leon-Garcia, "Autonomous demand-side management based on game-theoretic energy consumption scheduling for the future smart grid," *IEEE Trans. Smart Grid*, vol. 1, no. 3, pp. 320–331, Dec. 2010.

[5] Z. Zhou, C. Sun, R. Shi, Z. Chang, S. Zhou, and Y. Li, "Robust energy scheduling in vehicle-to-grid networks," *IEEE Netw.*, vol. 31, no. 2, pp. 30–37, Mar. 2017.

[6] Z. Zhou, J. Gong, Y. He, and Y. Zhang, "Software defined machine-to-machine communication for smart energy management," *IEEE Commun. Mag.*, vol. 55, no. 10, pp. 52–66, Oct. 2017.

[7] C. Wu, H. Mohsenian-Rad, and J. Huang, "Vehicle-to-aggregator interaction game," *IEEE Trans. Smart Grid*, vol. 3, no. 1, pp. 434–442, Mar. 2012.

[8] Z. Zhou, H. Yu, C. Xu, Y. Zhang, S. Mumtaz, and J. Rodriguez, "Dependable content distribution in D2D-based cooperative vehicular networks: A big data-integrated coalition game approach," *IEEE Trans. Intell. Transp. Syst.*, vol. 19, no. 3, pp. 953–964, Mar. 2018.

[9] E. L. Karfopoulos, K. A. Panourgias, and N. D. Hatziargyriou, "Distributed coordination of electric vehicles providing V2G regulation services," *IEEE Trans. Power Syst.*, vol. 31, no. 4, pp. 2834–2846, Jul. 2016.

[10] R. Yu, J. Ding, W. Zhong, Y. Liu, and S. Xie, "PHEV charging and discharging cooperation in V2G networks: A coalition game approach," *IEEE Internet Things J.*, vol. 1, no. 6, pp. 578–589, Dec. 2014.

[11] A. Dorri, M. Steger, S. S. Kanhere, and R. Jurdak, "Blockchain: A distributed solution to automotive security and privacy," *IEEE Commun. Mag.*, vol. 55, no. 12, pp. 119–125, Dec. 2017.

[12] W. L. Chin, W. Li, and H. H. Chen, "Energy big data security threats in IoT-based smart grid communications," *IEEE Commun. Mag.*, vol. 55, no. 10, pp. 70–75, Oct. 2017.

[13] Z. Liu, Z. Zhang, Y. Cao, Z. Xi, S. Jing, and H. L. Roche, "Towards a secure zero-rating framework with three parties," in *Proc. 27th USENIX Secur. Symp.*, Baltimore, MD, USA, Aug. 2018, pp. 718–728.

[14] K. M. S. Huq, S. Mumtaz, J. Rodriguez, P. Marques, B. Okyere, and V. Frascolla, "Enhanced c-ran using D2D network," *IEEE Commun. Mag.*, vol. 55, no. 3, pp. 100–107, Mar. 2017.

[15] W. Zhong, K. Xie, Y. Liu, C. Yang, and S. Xie, "Topology-aware vehicle-to-grid energy trading for active distribution systems," *IEEE Trans. Smart Grid*, to be published, doi: 10.1109/TSG.2018.2789940.

[16] S. Xie, W. Zhong, K. Xie, R. Yu, and Y. Zhang, "Fair energy scheduling for vehicle-to-grid networks using adaptive dynamic programming," *IEEE Trans. Neural Netw. Learn. Syst.*, vol. 27, no. 8, pp. 1697–1707, Aug. 2016.

[17] V. R. Tannahill, D. Sutanto, K. M. Muttaqi, and M. A. Masrur, "Future vision for reduction of range anxiety by using an improved state of charge estimation algorithm for electric vehicle batteries implemented with low-cost microcontrollers," *IET Electr. Syst. Transp.*, vol. 5, no. 1, pp. 24–32, Feb. 2015.

[18] Y. Wu, X. Tan, L. Qian, D. H. K. Tsang, W. Z. Song, and L. Yu, "Optimal pricing and energy scheduling for hybrid energy trading market in future smart grid," *IEEE Trans. Ind. Informat.*, vol. 11, no. 6, pp. 1585–1596, Dec. 2015.

[19] W. Zhong, K. Xie, Y. Liu, C. Yang, and S. Xie, "Auction mechanisms for energy trading in multi-energy systems," *IEEE Trans. Ind. Inf.*, vol. 14, no. 4, pp. 1511–1521, Apr. 2018.

[20] H. Liu, Y. Zhang, and T. Yang, "Blockchain-enabled security in electric vehicles cloud and edge computing," *IEEE Netw.*, vol. 32, no. 3, pp. 78–83, May 2018.

[21] Z. Li, J. Kang, R. Yu, D. Ye, Q. Deng, and Y. Zhang, "Consortium blockchain for secure energy trading in industrial internet of things," *IEEE Trans. Ind. Informat.*, vol. 14, no. 8, pp. 3690–3700, Aug. 2018.

[22] M. Tariq, P. K. Yong, J. H. Kim, J. P. Yong, and E. H. Jung, "Energy efficient and reliable routing scheme for wireless sensor networks," in *Proc. Int. Conf. Commun. Softw. Netw.*, Macau, China, Feb. 2009, pp. 181–185.

[23] J. Kang, R. Yu, X. Huang, S. Maharjan, Y. Zhang, and E. Hossain, "Enabling localized peer-to-peer electricity trading among plug-in hybrid electric vehicles using consortium blockchains," *IEEE Trans. Ind. Informat.*, vol. 13, no. 6, pp. 3154–3164, Dec. 2017.

[24] L. Duan, L. Gao, and J. Huang, "Cooperative spectrum sharing: A contract-based approach," *IEEE Trans. Mobile Comput.*, vol. 13, no. 1, pp. 174–187, Jan. 2014.

[25] Y. Zhang, L. Song, W. Saad, Z. Dawy, and Z. Han, "Contract-based incentive mechanisms for device-to-device communications in cellular networks," *IEEE J. Sel. Areas Commun.*, vol. 33, no. 10, pp. 2144–2155, Oct. 2015.

[26] T. Liu, J. Li, F. Shu, M. Tao, W. Chen, and Z. Han, "Design of contract-based trading mechanism for a small-cell caching system," *IEEE Trans. Wireless Commun.*, vol. 16, no. 10, pp. 6602–6617, Oct. 2017.

[27] G. O. Sahinoglu, M. Pajovic, Z. Sahinoglu, Y. Wang, P. V. Orlik, and T. Wada, "Battery state-of-charge estimation based on regular/recurrent Gaussian process regression," *IEEE Trans. Ind. Electron.*, vol. 65, no. 5, pp. 4311–4321, May 2018.

[28] C. Huang and L. Wang, "Gaussian process regression-based modelling of lithium-ion battery temperature-dependent open-circuit-voltage," *Electron. Lett.*, vol. 53, no. 17, pp. 1214–1216, Sep. 2017.

[29] K. S. Ng, C. S. Moo, Y. P. Chen, and Y. C. Hsieh, "Enhanced coulomb counting method for estimating state-of-charge and state-of-health of lithium-ion batteries," *Appl. Energy*, vol. 86, no. 9, pp. 1506–1511, Sep. 2009.

[30] Z. Chen, Y. Fu, and C. C. Mi, "State of charge estimation of lithium-ion batteries in electric drive vehicles using extended Kalman filtering," *IEEE Trans. Veh. Technol.*, vol. 62, no. 3, pp. 1020–1030, Mar. 2013.

[31] M. Charkhgard and M. Farrokhi, "State-of-charge estimation for lithium-ion batteries using neural networks and EKF," *IEEE Trans. Ind. Electron.*, vol. 57, no. 12, pp. 4178–4187, Dec. 2010.

[32] J. A. Anton, P. J. G. Nieto, C. B. Viejo, and J. A. V. Vilan, "Support vector machines used to estimate the battery state of charge," *IEEE Trans. Power Electron.*, vol. 28, no. 12, pp. 5919–5926, Dec. 2013.
[33] D. Liu, J. Pang, J. Zhou, Y. Peng, and M. Pecht, "Prognostics for state of health estimation of lithium-ion batteries based on combination Gaussian process functional regression," *Microelectron. Rel.*, vol. 53, no. 6, pp. 832–839, Apr. 2013.
[34] G. Ozcan, M. Pajovic, Z. Sahinoglu, Y. Wang, P. V. Orlik, and T. Wada, "Online battery state-of-charge estimation based on sparse Gaussian process regression," in *Proc. IEEE Power Energy Soc. Gen. Meet*, Boston, MA, USA, Jul. 2016, pp. 1–5.
[35] G. C. Hsieh, L. R. Chen, and K. S. Huang, "Fuzzy-controlled li-ion battery charge system with active state-of-charge controller," *IEEE Trans. Ind. Electron.*, vol. 48, no. 3, pp. 585–593, Jun. 2001.
[36] T. Lipp and S. Boyd, "Variations and extension of the convex-concave procedure," *Optim. Eng.*, vol. 17, no. 2, pp. 263–287, Jun. 2016.
[37] X. Li, M. Li, Y. J. Gong, X. L. Zhang, and J. Yin, "T-DesP: Destination prediction based on big trajectory data," *IEEE Trans. Intell. Transp. Syst.*, vol. 17, no. 8, pp. 2344–2354, Aug. 2016.
[38] C. E. Rasmussen and C. K. I. Williams, *Gaussian Processes for Machine Learning.* Cambridge, MA, USA: MIT Press, 2006.
[39] D. C. Aishwarya and C. N. Babu, "Prediction of time series data using gabpnn based hybrid ann model," in *Proc. Adv. Comput. Conf.*, Hyderabad, India, Jul. 2017, pp. 848–853.
[40] Y. A. U. Rehman, M. Tariq, and T. Sato, "A novel energy efficient object detection and image transmission approach for wireless multimedia sensor networks," *IEEE Sensors J.*, vol. 16, no. 15, pp. 5942–5949, Aug. 2016.

Zhenyu Zhou (M'11–SM'17) received the M.E. and Ph.D. degrees from Waseda University, Tokyo, Japan, in 2008 and 2011, respectively. From April 2012 to March 2013, he was the Chief Researcher with the Department of Technology, KDDI, Tokyo, Japan. Since March 2013, he is an Associate Professor with the School of Electrical and Electronic Engineering, North China Electric Power University, Beijing, China. His research interests include green communications, vehicular communications, and smart grid communications. He served as an Associate Editor for IEEE ACCESS, *EURASIP Journal on Wireless Communications and Networking*, a Guest Editor for IEEE COMMUNICATIONS MAGAZINE and *Transactions on Emerging Telecommunications Technologies*. He also served as workshop co-chair for IEEE Globecom 2018, IEEE ISADS 2015, and TPC member for IEEE Globecom, IEEE CCNC, IEEE ICC, IEEE APCC, IEEE VTC, IEEE Africon, etc. He is a voting member of IEEE Standard Association P1932.1 Working Group. He was the recipient of the IEEE Vehicular Technology Society "Young Researcher Encouragement Award" in 2009, the Beijing Outstanding Young Talent Award in 2016, the IET Premium Award in 2017, the IEEE Comsoc Green Communications and Computing Technical Committee (IEEE GCCTC) 2017, 2018 Best Paper Award, and IEEE Globecom Best Paper Award 2018.

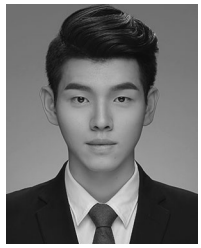

Bingchen Wang is currently working toward the B.S. degree with North China Electric Power University, Beijing, China. His research interests include green communications and smart grid.

Yufei Guo is currently working toward the M.S. degree with North China Electric Power University, Beijing, China. His research interests include green communications and smart grid.

Yan Zhang (M'05–SM'10) received the Ph.D. degree from the School of Electrical and Electronics Engineering, Nanyang Technological University, Singapore. He is a Full Professor with the Department of Informatics, University of Oslo, Oslo, Norway. His current research interests include next-generation wireless networks leading to 5G, green, and secure cyber-physical systems. He is an Associate Technical Editor of IEEE COMMUNICATIONS MAGAZINE, an Editor of IEEE TRANSACTIONS ON GREEN COMMUNICATIONS AND NETWORKING, an Editor of IEEE COMMUNICATIONS SURVEYS AND TUTORIALS, and an Associate Editor of IEEE ACCESS. He serves as chair positions in a number of conferences, including IEEE GLOBECOM 2017, IEEE PIMRC 2016, IEEE CloudCom 2016, etc. He serves as TPC member for numerous international conference including IEEE INFOCOM, IEEE ICC, etc. He is IEEE Vehicular Technology Society Distinguished Lecturer. He is also a senior member of IEEE ComSoc, IEEE CS, IEEE PES, and IEEE VT society. He is a Fellow of IET.